Electrical properties of the fast-ion conductor lanthanum fluoride

John R Igel†, Mary C Wintersgill†, John J Fontanella†, Alan V Chadwick‡, Carl G Andeen§ and Vern E Bean∥

† Physics Department, US Naval Academy, Annapolis, MD 21402, USA
‡ Chemistry Department, University of Kent, Canterbury, Kent, UK
§ Physics Department, Case Western Reserve University, Cleveland, OH 44106, USA
∥ National Bureau of Standards, Washington, DC 20234, USA

Abstract. Audio-frequency complex-impedance measurements have been performed on pure and alkaline-earth-doped lanthanum trifluoride at zero pressure over the temperature range 5.5–310 K and at pressures up to 0.3 GPa in the vicinity of room temperature. Studies have been made both parallel and perpendicular to the optical axis. The real part of the dielectric constant is found to be given by $\varepsilon'_\| \simeq 12.6$ and $\varepsilon'_\perp \simeq 14.4$ and both components increase slightly with temperature.

Also, for the calcium-doped material, four relaxations have been observed. The activation enthalpy for the principal relaxation is close to that for the motion of free vacancies and thus is attributable to the reorientation of a bound vacancy. In addition, the anisotropy ratio for the relaxation is found to be $A_\perp/A_\| \simeq 1.8$, which is opposite to the anisotropy observed for DC conductivity. An explanation of the anisotropy ratio is discussed. The remaining relaxations are tentatively attributed to other jumps of bound vacancies.

Finally, the pressure-dependent conductivity has been measured in the association region, yielding an activation volume of about 2.4 cm³ mol⁻¹. The value parallel to the optical axis is slightly larger than that perpendicular to the optical axis. In addition, the thermal expansion coefficient of the activation volume is found to be negative. The value of 2.4 cm³ mol⁻¹ is interpreted to be the activation volume for the motion of vacancies.

1. Introduction

The electrical properties of lanthanum trifluoride are rather interesting. Early studies (Sher *et al* 1966, 1967, Solomon *et al* 1966, Goldman and Shen 1966, Lee and Sher 1965) showed anomalously large polarisation effects and fast-ion motion. The latter effect has motivated more recent studies (Chadwick *et al* 1979, Schoonman *et al* 1980, Fontanella *et al* 1981b) aimed at a better understanding of the conduction mechanisms.

The present work consists of low-temperature and high-pressure conductivity studies which provide more information concerning ion transport in lanthanum trifluoride. The fact that low-temperature studies provide information that is complementary to the high-temperature conductivity work is shown in figure 1 where the results of both high- and low-temperature studies on a commercially grown 'pure' sample are given. The high-temperature results for a pure sample grown in our own laboratory are also
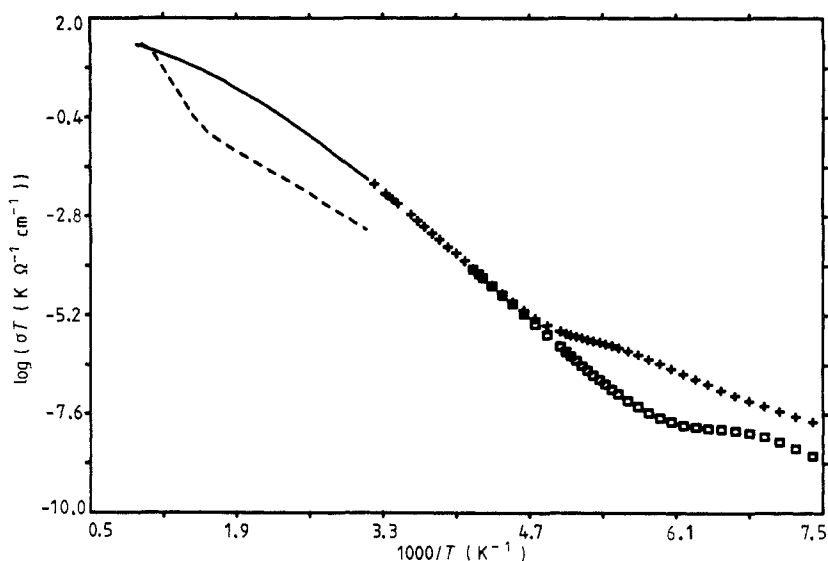
Figure 1. $\log(\sigma T(\mathrm{K}\ \Omega^{-1}\ \mathrm{cm}^{-1}))$ against $1000/T(\mathrm{K}^{-1})$ perpendicular to the c axis for two samples of pure lanthanum trifluoride. Broken curve: grown by the authors; full curve: $+$ (10^4 Hz), $\square$ (10^2 Hz), commercial source. The curves connect the datum points.

shown. The difference between the two 'pure' materials is obvious. However, the low-temperature results show the reason for the difference between the two materials in that a relaxation is observed in the commercial sample, indicating a significant impurity level. Thus in addition to merely extending the range of the conductivity studies, low-temperature work provides a direct observation of impurities. Also, figure 1 emphasises the need for a systematic study of carefully prepared samples. Finally, high-pressure studies are useful as they allow the determination of activation volumes.

In the present work, a systematic study of calcium-doped lanthanum trifluoride is reported, and several new results are obtained.

2. Experimental procedure

Some pure and some calcium-doped lanthanum trifluoride crystals were obtained from Optovac Inc., and others were grown using the Stockbarger method (Figueroa *et al* 1978). The crystals tended to grow with the optical axis perpendicular to the long axis of the cylindrical boules. To check for any concentration gradients, the Optovac samples used for determining the complex dielectric constant perpendicular to the c axis, $\varepsilon_{\perp}^{*} = \varepsilon_{\perp}' - i\varepsilon_{\perp}''$, were cut from both the top and the bottom of each boule. These samples were discs approximately 8 mm in diameter and about 1 mm thick. The samples grown in our laboratory were discs about 2 mm in diameter and 1 mm thick. Aluminium was evaporated onto the faces yielding a two-terminal capacitor.

For measurements parallel to the c axis,

$$\varepsilon_{\parallel}^{*} = \varepsilon_{\parallel}' - i\varepsilon_{\parallel}''$$

the Optovac samples were cut from the centre of the boule and were platelets of approximate size $9 \times 11 \times 1$ mm^3. The orientation was checked using crossed polaroids.

Some of these samples were evaporated in the standard three-terminal configuration. The samples grown in our laboratory were smaller, being $6 \times 9 \times 1$ mm^3 platelets.

All of the impedance measurements were performed using a fully automated microprocessor-controlled impedance bridge operating at the five frequencies 10^2, $10^{2.5}$, 10^3, $10^{3.5}$ and 10^4 Hz. Temperatures from 5.5 to 310 K were achieved in a Cryogenics Associates CT-14 cryostat with an eight-sample holder.

The resulting values of capacitance C, and the conductance divided by the angular frequency, G/ω, were transformed to the complex dielectric constant as follows.

First, the values of the dielectric constants at 300 K and 1000 Hz were determined using standard geometrical techniques in which the capacitance is assumed to be given by the usual expression for a parallel-plate capacitor:

$$C = \varepsilon' \varepsilon_0 S/d \tag{1}$$

where S is the area of the plates, d is their separation, and ε_0 is the permittivity of free space. In cases where two-terminal measurements were performed, the area was determined both by direct measurement and by a combination of mass, density (Swanson *et al* 1957) and thickness measurements. The values always agreed within 2%. In the case of three-terminal measurements, the area was determined from the area of the guarded electrode on the crystal face.

For measurements parallel to the c axis, the real part of the dielectric constant was calculated from the data using the equation

$$\varepsilon'_{\parallel}/(\varepsilon'_{\parallel})_{300} = (C_T/C_{300}) \exp(-A') \tag{2a}$$

where

$$A' = \int_{300}^{T} (2\alpha_{\perp} - \alpha_{\parallel}) \, \mathrm{d}T \tag{2b}$$

and where $\alpha_{\perp}$ and $\alpha_{\parallel}$ are the linear isobaric thermal expansion coefficients perpendicular and parallel to the c axis respectively.

For measurements perpendicular to the c axis, the real part of the dielectric constant was calculated using

$$\varepsilon'_{\perp}/(\varepsilon'_{\perp})_{300} = (C_T/C_{300}) \exp(-B') \tag{3a}$$

where

$$B' = \int_{300}^{T} \alpha_{\parallel} \, \mathrm{d}T. \tag{3b}$$

The thermal expansion coefficients for lanthanum trifluoride were approximated by scaling the room-temperature values quoted by Mooney (1966) to the published low-temperature data for BaF$_2$ (Bailey and Yates 1967). The approximate values for the thermal expansion correction factors are listed in table 1, together with the average values of the dielectric constant at various temperatures. The actual low-temperature dielectric constants for various samples are listed in table 2.

Finally, the values of ε'' and the conductivity, σ, for each temperature were calculated from

$$\varepsilon'' = G\varepsilon'/\omega C \tag{4}$$

and

$$\sigma = \varepsilon_0 \varepsilon'' \omega. \tag{5}$$

Table 1. Values of the dielectric constant and thermal expansion correction factor for lanthanum trifluoride.

T(K)	$A'(\times 10^{-3})$	$\varepsilon'_{\parallel}$	$B'(\times 10^{-3})$	$\varepsilon'_{\perp}$
5.5	3.892	12.6	2.078	14.4
25	3.890	12.600	2.077	14.403
40	3.874	12.603	2.069	14.411
50	3.849	12.607	2.055	14.422
60	3.807	12.612	2.033	14.436
70	3.748	12.619	2.001	14.450
80	3.673	12.627	1.961	14.467
90	3.582	12.637	1.913	14.486
100	3.477	12.649	1.857	14.509
110	3.360	12.660	1.794	14.531
120	3.232	12.672	1.726	14.554
130	3.095	12.685	1.653	14.577
140	2.949	12.698	1.575	14.601
150	2.797	12.701	1.493	14.625
160	2.637	12.725		

Table 2. 5.5 K dielectric constant for various samples.

Concentration (%)	$\varepsilon'_{\parallel}$	$\varepsilon'_{\perp}$
Optovac, Inc.		
Pure	12.5	14.0
0.01	12.5	14.4
		13.3
0.03	13.1	14.3
		14.9
0.1	12.7	13.6
		15.0
0.3	12.4	13.9
		15.1
		13.9
		14.7
Grown by the authors		
Pure	13.5†	16.0†
0.1	13.3†	16.2†

† Poor boundary conditions due to small sample size.

Hydrostatic pressures up to 0.3 GPa at 274, 279.5 and 285.4 K were generated using an Enerpac pump and Spinesstic 38 (current nomenclature is Spinesstic 22) as the pressure-transmitting fluid. The pressure bomb and multiple-sample holder were similar to those described elsewhere (Fontanella *et al* 1972). In the present work the pressures were measured using a Heise Bourdon tube gauge.

3. Discussion

3.1. ε'' and σ against temperature

3.1.1. Electrode effects. Typical results for the imaginary part of the dielectric constant (AC conductivity) are shown in figure 2 for alkaline-earth-doped lanthanum trifluoride. Three regions are apparent. Above about 250 K there is a region where the conductivity appears to depend strongly on frequency. For example, a peak is observed in log σT against $1000/T$. The corresponding effect in the real part of the dielectric constant is shown in figure 3. Because of the nature of the strength and frequency dependence of this apparent relaxation, it is attributed to blocking electrode effects and will not be discussed further in this paper.
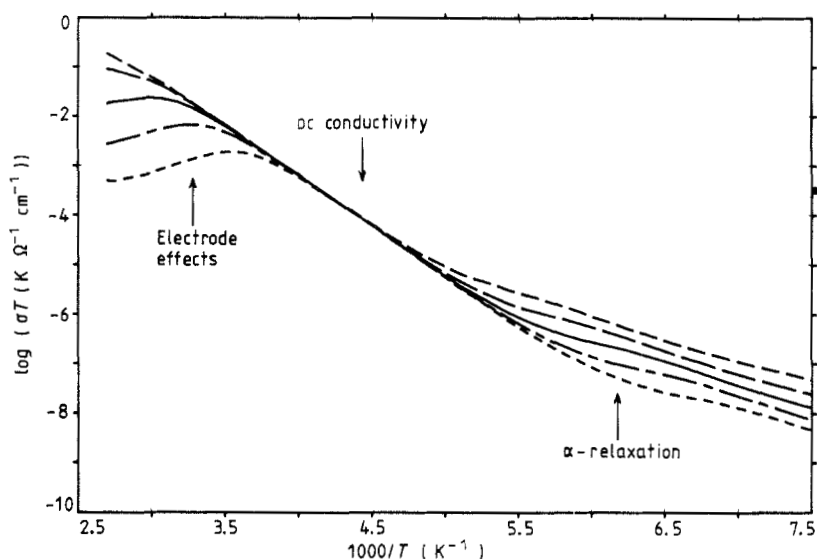

Figure 2. $\log(\sigma T(\mathrm{K}\,\Omega^{-1}\,\mathrm{cm}^{-1}))$ against $1000/T(\mathrm{K}^{-1})$ perpendicular to the c axis for 1.0 mol% calcium-doped lanthanum trifluoride grown by the authors. The curves connect the datum points and the curves from bottom to top are for 10^2, $10^{2.5}$, 10^3, $10^{3.5}$ and 10^4 Hz.

3.1.2. α-relaxation and DC conductivity. Below about 250 K is a region with a relaxation (α) superimposed on the DC conductivity. While the relaxation is not prominent in the 1.0% calcium-doped material, it is particularly visible in the less heavily doped material as shown in figures 4 and 5. The relaxation is attributed to jumps of a bound vacancy about a substitutional alkaline-earth ion.

The contribution of the DC conductivity is modelled by

$$\sigma T = \sigma_0 \exp(-E'/kT) \tag{6}$$

where σ_0 and E' are adjustable parameters and k is the Boltzmann constant. Further,

$$E' = h_m^f + h_a/2 \tag{7}$$

where h_m^f is the migration enthalpy of a free vacancy and h_a is the average association enthalpy for a vacancy bound to an alkaline-earth ion.
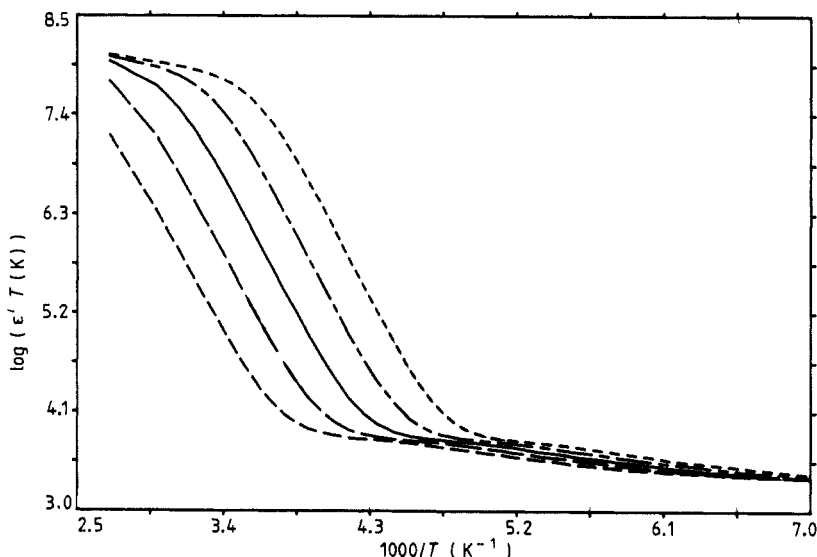
Figure 3. $\log(\varepsilon'T(\mathrm{K}))$ against $1000/T(\mathrm{K}^{-1})$ perpendicular to the c axis for $1.0\,\mathrm{mol\%}$ calcium-doped lanthanum trifluoride grown by the authors. The curves connect the datum points and the curves from bottom to top are for 10^4, $10^{3.5}$, 10^3, $10^{2.5}$ and 10^2 Hz.

Next, the relaxation was modelled using the Cole–Cole expression (Smyth 1955):

$$\sigma T = \varepsilon_0 \omega A \cos(\alpha\pi/2)/2\{\cosh[(1 - \alpha)x] + \sin(\alpha\pi/2)\} \tag{8}$$

where α is the Cole–Cole parameter which is a measure of the broadening of the relaxation peak, A is a measure of the dipole strength, and $x = \ln(\omega\tau)$ where

$$\tau = \tau_0 \exp(h_\mathrm{m}^\mathrm{b}/kT). \tag{9}$$

τ_0 is the constant pre-exponential factor and h_m^b is the enthalpy for the motion of bound vacancies.

The best fit of this expression to the data was found using techniques described elsewhere (Kimble *et al* 1982). The results of the fitting procedure are given in tables 3 and 4 and examples are shown in figures 4 and 5. Several features are evident.

The first result is that the strength of the relaxation, A, increases with the concentration of calcium. This implies that the dipolar complex is associated with single calcium ions. Next, the reorientation energy for the dipolar complex is approximately 0.3 eV. This value is close to the value for free-vacancy migration, 0.28 eV, reported by Chadwick *et al* (1979). Schoonman *et al* (1980) report a value of 0.27 eV for conductivity over the temperature range 400–525 K. This supports the identification of the dipolar complex as a vacancy bound at a substitutional calcium ion, as it is expected from work on other fluorides that the motional enthalpies should be similar. That is because the sizes of identically coordinated trivalent lanthanum ions and divalent calcium ions are about the same (Shannon 1976), the lanthanum ion being slightly larger. It has been found in other fluorides that motional enthalpies for bound and free vacancies are very close to one another when the size of the substitutional matches that of the host (Fontanella *et al* 1980, Wintersgill *et al* 1980, Fontanella *et al* 1981b).

Next, the values of E' can be used to obtain an association energy. The average value of E' perpendicular to the c axis is 0.51 eV and that parallel is 0.47 eV. This trend is in

agreement with the results of Schoonman *et al* (1980) who report values of 0.46 and 0.44 eV for perpendicular and parallel activation energies, respectively, for conductivity of LaF$_3$ over the temperature range 290–400 K. In the present work, the difference in the values of E' is attributed to the difference in h_m^f since h_a should be the same both parallel and perpendicular to the c axis.

Figure 4. $\log(\sigma T(\text{K }\Omega^{-1}\text{ cm}^{-1}))$ against $1000/T(\text{K}^{-1})$ parallel to the c axis for 0.3 mol% calcium-doped lanthanum trifluoride grown by Optovac, Inc. The best-fit curves are shown along with the datum points: $\triangle$ 10^2 Hz; $\diamond$ 10^3 Hz; $\square$ 10^4 Hz. Two intermediate frequencies, $10^{2.5}$ and $10^{3.5}$ Hz, are not shown.

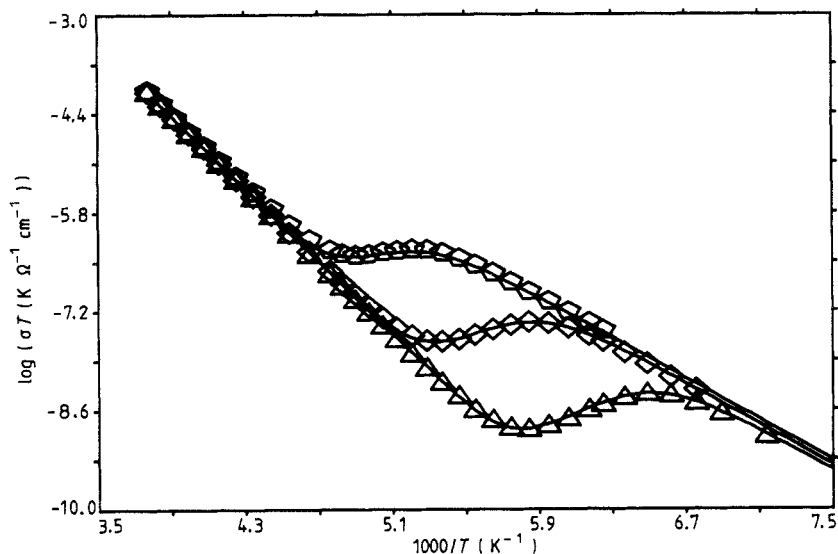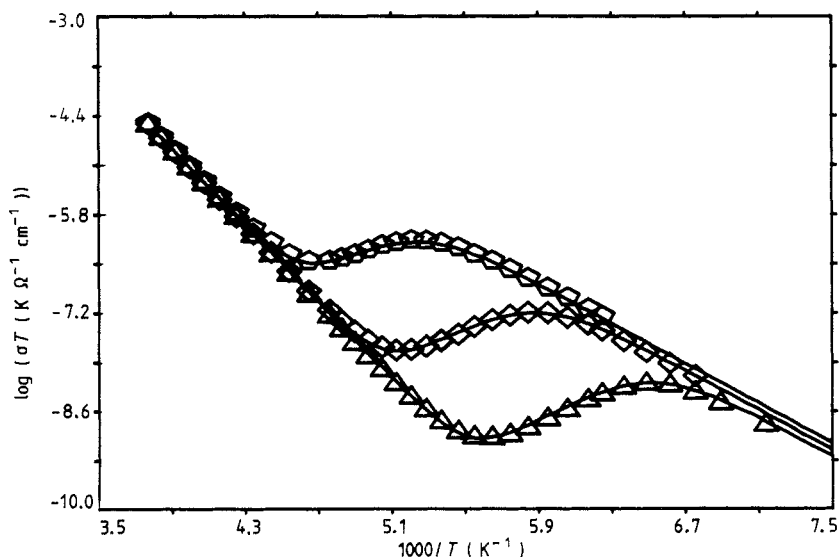**Figure 5.** $\log(\sigma T(\text{K }\Omega^{-1}\text{ cm}^{-1}))$ against $1000/T(\text{K}^{-1})$ perpendicular to the c axis for 0.3 mol% calcium-doped lanthanum trifluoride grown by Optovac, Inc. The best-fit curves are shown along with the datum points: $\triangle$ 10^2 Hz; $\diamond$ 10^3 Hz; $\square$ 10^4 Hz. Two intermediate frequencies, $10^{2.5}$ and $10^{3.5}$ Hz, are not shown.

This is supported by the values of h_m^b in tables 3 and 4 since the enthalpy for motion parallel to the c axis is slightly smaller than motion perpendicular to the c axis, the average of the perpendicular values being 0.32 eV and the average parallel value being 0.31 eV. Considering the value for h_m^f of 0.28 eV given by Chadwick *et al* (1979), it is concluded that a reasonable set of h_m^f values are 0.31 and 0.29 eV for motion perpendicular and parallel to the c axis, respectively. These lead to an average value of about 0.38 eV for the association energy for vacancies bound to a calcium ion.

Table 3. Best-fit parameters for the α-relaxation and association-region DC conductivity in calcium-doped lanthanum trifluoride parallel to the c axis.

Concentration (%)	E'(eV)	$\ln(\sigma_0(K\,\Omega^{-1}\,cm^{-1}))$	h_m^{bv}(eV)	$\tau_0(10^{-14}\,s)$	A(K)	α	RMS deviation
Optovac, Inc.							
0.01	0.457	11.0	0.310	9.29	14.8	0.06	0.011
0.03	0.457	10.8	0.302	16.1	20.0	0.05	0.014
0.1	0.462	11.2	0.309	11.6	121.6	0.10	0.028
0.3	0.512	13.0	0.309	11.6	174.3	0.07	0.020
Grown by the authors							
0.1	0.452	11.2	0.304	15.9	82.0	0.13	0.028

Table 4. Best-fit parameters for the α-relaxation and association-region DC conductivity in calcium-doped lanthanum trifluoride perpendicular to the c axis.

Concentration (%)	E'(eV)	$\ln(\sigma_0(K\,\Omega^{-1}\,cm^{-1}))$	h_m^{bv}(eV)	$\tau_0(10^{-14}\,s)$	A(K)	α	RMS deviation
Optovac, Inc.							
0.01	0.506	11.8	0.335	1.61	29.1	0.10	0.023
	0.506	11.7	0.335	1.57	30.5	0.09	0.026
0.03	0.518	12.4	0.331	2.29	39.8	0.12	0.029
0.1	0.488	11.0	0.312	9.16	218	0.13	0.024
(Bottom)	0.478	11.3	0.304	16.7	204	0.11	0.026
0.3	0.546	13.6	0.302	18.4	261	0.09	0.024
	0.537	13.1	0.311	9.9	267	0.09	0.017
	0.536	13.1	0.310	10.0	274	0.09	0.018
(Bottom)	0.527	12.7	0.311	9.5	230	0.08	0.016
Grown by the authors							
0.1	0.485	11.1	0.309	13.9	144	0.20	0.036

Next, it is interesting that the anisotropy ratio for the strength of the dielectric relaxation is opposite to that for the conductivity. That is, it is found that

$$A_\perp \simeq 1.8\,A_\parallel$$

in contrast to the result that $\sigma_\parallel \simeq 2\sigma_\perp$ (Chadwick *et al* 1979, Schoonman *et al* 1980).

To be sure that this was not due to a concentration gradient in the crystal, measurements perpendicular to the c axis were made on samples taken from both the bottom and the top of the boule, and, for measurements parallel to the c axis, the samples were taken from the centre of the boule, as mentioned above. While some variations are noted, the strength of the relaxation perpendicular to the c axis is certainly always larger than that parallel to the c axis by about this factor.

This result can be understood qualitatively as follows. Zalkin *et al* (1966) have shown that La is approximately ninefold-coordinated with fluorines at slightly different distances from the lanthanum ion (F(1), F(2), and F(3)). Those fluorines are shown in figure 6 and are relabelled 1–9 for the purposes of the present work.

Figure 6. Substitutional calcium (full circle) and nine nearest-neighbour fluorine positions. The structure is that given by Zalkin *et al* (1966). The nearest-neighbour positions are renumbered for the purpose of the present work and the numbers in parentheses are the fractional distances along the *c* axis. Also shown are the fluorine–calcium distances.

On the basis of an undistorted point-ion model, if a calcium ion substitutes for a lanthanum, fluorine vacancies at sites 5 and 6 will be most energetically favourable. Specifically, those sites are 0.1, 0.17 and 0.5 eV more favourable than the three other pairs of equivalent sites, 1–7, 2–9 and 4–8, respectively. The important fact is that 5–6 will give a relaxation perpendicular to the optical axis only. Further, the relaxation may take place via site 4 since the jump distances 5–4 and 4–6 are rather short as can be seen from table 5, where the undistorted inter-ionic distances are tabulated for the nine nearest-neighbour fluorines.

However, the point-ion model is insufficient to explain the contribution parallel to the optic axis at the intensity observed. This relaxation may be due to distortion of sites

Table 5. Inter-ionic distances for lanthanum trifluoride in Å and using the notation of figure 6.

Site	1	2	3	4	5	6	7	8	9
1	—	2.55	3.32	2.92	3.18	3.14	4.81	4.54	4.29
2		—	2.58	4.22	2.56	4.76	4.29	4.93	4.61
3			—	5.08	4.17	4.17	3.32	5.07	2.58
4				—	2.56	2.61	4.54	2.49	4.92
5					—	4.15	3.78	3.02	5.00
6						—	3.82	2.98	2.98
7							—	2.92	2.55
8								—	4.22

5 and 6 because of the presence of the aliovalent ion, resulting in a shift of the z coordinate of one or both of the ions.

Alternatively, $A_\perp \simeq 1.8 A_\parallel$ could be explained if a second relaxation has an activation energy of about 0.3 eV and has a component parallel to the optical axis. For example, there may be a contribution from the 3–2–5 reorientation although this clearly represents an inequivalent well problem.

In summary then, the results for the principal relaxation can be explained qualitatively. A more quantitative explanation, including a test of the above arguments, could be obtained via computer calculations such as HADES.

3.1.3. Other relaxations. Below 150 K three other relaxations are observed parallel to the c axis and two others are observed perpendicular to the c axis. They are labelled β, γ and δ in order of decreasing temperature or activation enthalpy. Their approximate strengths and positions are given in table 6. It is interesting that the δ-relaxation is only

Table 6. Approximate strengths of the relaxations found in calcium-doped lanthanum trifluoride. The α-, β-, γ- and δ-relaxations occur at about 180, 85, 60 and 15 K, respectively, at 1000 Hz.

Concentration (%)	α	β	γ	δ
Parallel to the c axis				
Optovac, Inc.				
0.01	15	0.03		
0.03	20	0.03		0.006
0.1	122	0.19	0.05	0.018
0.3	174	0.31		0.024
1.0		1.7	0.6	0.12
Grown by the authors				
0.1	82	0.068		0.005
1.0		1.4	0.12	0.09
Perpendicular to the c axis				
Optovac, Inc.				
0.01	30	0.44		
0.03	40			
0.1	210	0.56	0.06	
0.3	260	0.17	0.05	
1.0		1.02	0.72	
Grown by the authors				
0.1	144	0.21		
1.0		0.85	0.24	0.024†

† Attributed to improper orientation.

observed parallel to the c axis. This is, of course, not unusual and gives important information concerning the site symmetry for that defect complex (Nowick 1967). It is felt that all of these relaxations are associated with calcium impurities as all are observed in *both* the Optovac samples and those grown by the authors. The existence of multiple relaxations is not surprising in view of the complex structure of lanthanum trifluoride.

No attempt will be made in the present paper to identify these complexes as further work is necessary. Clearly, mechanical relaxation studies would be particularly useful.

3.2. *Conductivity against pressure*

Next, the effect of high pressure on the conductivity was determined in the association region for the crystals grown by the authors. Typical results are shown in figure 7 and the best-fit slopes to the data are given in table 7. The results were transformed to activation volumes as follows.
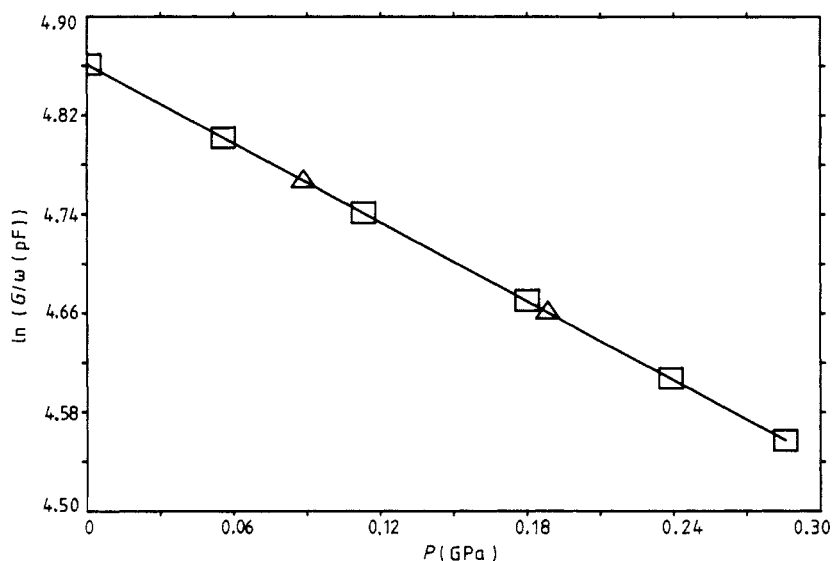
Figure 7. $\ln(G/\omega(\text{pF}))$ against $P(\text{GPa})$ parallel to the c axis for 0.1 mol% calcium-doped lanthanum trifluoride grown by the authors. The measurements were at 274 K. The datum points are shown along with the best-fit straight line: $\square$ decreasing pressure; $\triangle$ increasing pressure.

Table 7. Results of the effect of pressure on the DC conductivity in the association region for calcium-doped lanthanum trifluoride grown by the authors.

Orientation	$T(\text{K})$	$-(\partial \ln G/\partial P)\,(\text{GPa})^{-1}$	$-(\partial \ln \sigma/\partial P)\,(\text{GPa})^{-1}$	$V(\text{cm}^3\,\text{mol}^{-1})$
Parallel to the	285.4	1.015	1.011	2.34
c axis	279.5	1.041	1.037	2.35
	274.0	1.064	1.060	2.36
Perpendicular	285.4	0.996	0.992	2.30
to the c axis	279.5	1.018	1.014	2.30
	274.0	1.036	1.032	2.30

The expression for the conductivity of a parallel-plate capacitor leads to the relations

$$(\mathrm{d}\ln \sigma_{\parallel}/\mathrm{d}P)|_T = (\mathrm{d}\ln G_{\parallel}/\mathrm{d}P)|_T - d_{\parallel} + 2d_{\perp} \tag{10}$$

and

$$(\mathrm{d}\ln \sigma_{\perp}/\mathrm{d}P)|_T = (\mathrm{d}\ln G_{\perp}/\mathrm{d}P)|_T + d_{\parallel} \tag{11}$$

where $G_\parallel$ and $G_\perp$ are the conductances and $d_\parallel$ and $d_\perp$ are the linear compressibilities parallel and perpendicular to the c axis. Since compressibilities for lanthanum trifluoride do not seem to be available, the linear compressibilities will be approximated by $\chi_T/3$ for calcium fluoride, where χ_T is the isothermal compressibility (Andeen *et al* 1972). As the correction factor is small, little error will be introduced by this approximation. The resultant values of the pressure derivatives of the conductivity are listed in table 7.

Next, to get the activation volume, it is assumed that

$$\sigma = (\sigma_0'/T) \exp(-g/kT) \tag{12}$$

where σ_0' is a new pre-exponential and g is the Gibbs energy. Thus, the activation volume is

$$V = (dg/dP)|_T = kT[(d\ln \sigma_0'/dP)|_T - (d\ln \sigma/dP)|_T]. \tag{13}$$

Further, assuming that the dominant pressure-dependent contribution to the first term is an attempt frequency ($\sigma_0' \equiv \text{constant} \times \nu_a$), it follows that

$$V = kT[\chi_T\gamma_a - (d\ln \sigma/dP)|_T] \tag{14}$$

where

$$\gamma_a = -(d\ln \nu_a/d\ln V)|_T \tag{15}$$

is the attempt mode Gruneisen parameter. Using an approximate value of 2.5 for the Gruneisen parameter (which is typical for the alkaline-earth fluorides, for example) the values of the activation volume calculated using equation (14) are listed in table 7.

The value of $2.4 \text{ cm}^3 \text{ mol}^{-1}$ is similar to that observed for vacancy motion in the alkaline-earth fluorides (Fontanella *et al* 1981a) and thus it is concluded that the vacancy transport mechanism is similar in lanthanum fluoride and the alkaline earth fluorides.

It is also noted that the activation volume for motion parallel to the c axis decreases with increasing temperature while for motion perpendicular to the c axis it is approximately constant. The negative thermal expansion coefficient for the activation volume is similar to that observed for bound-vacancy motion in the alkaline-earth fluorides (Fontanella *et al* 1981a).

3.3. The dielectric constant

The measurements for the real part of the dielectric constant indicate that

$$\varepsilon_\parallel' = 12.6 \pm 0.6 \qquad \varepsilon_\perp' = 14.4 \pm 0.6.$$

This is in reasonable agreement with the average value of 14 quoted by Mooney (1966).

A check of the anisotropy can be made via the Lyddane–Sachs–Teller relation for anisotropic crystals (Barker 1975, Cochran and Cowley 1962, Kurosawa 1961):

$$\frac{\varepsilon'}{\varepsilon_\infty'} = \prod_i \frac{\omega_{Li}^2}{\omega_{Ti}^2}. \tag{(16)}$$

Using the values for the infrared-active phonon frequencies measured by Lowndes *et al* (1969), the products are found to be

$$\prod_i \frac{\omega_{Li}^2}{\omega_{Ti}^2}\bigg|_\parallel = 4.65$$

and

$$\prod_i \frac{\omega_{Li}^2}{\omega_{Ti}^2}\bigg|_\perp = 5.00.$$

Since

$$(\varepsilon'_\infty)_\parallel \simeq (\varepsilon'_\infty)_\perp \simeq 2.56$$

(Mooney 1966), the generalised LST relation yields $\varepsilon'_\parallel = 11.9$ and $\varepsilon'_\perp = 12.8$ which confirms the measured anisotropy.

Finally, the temperature variation of the dielectric constant has been measured. Typical results are shown in figure 8 where a small positive temperature coefficient is seen. Values for the dielectric constant at various temperatures are listed in table 1. The variation with temperature is slightly smaller than for the alkaline-earth fluorides (Andeen *et al* 1972).
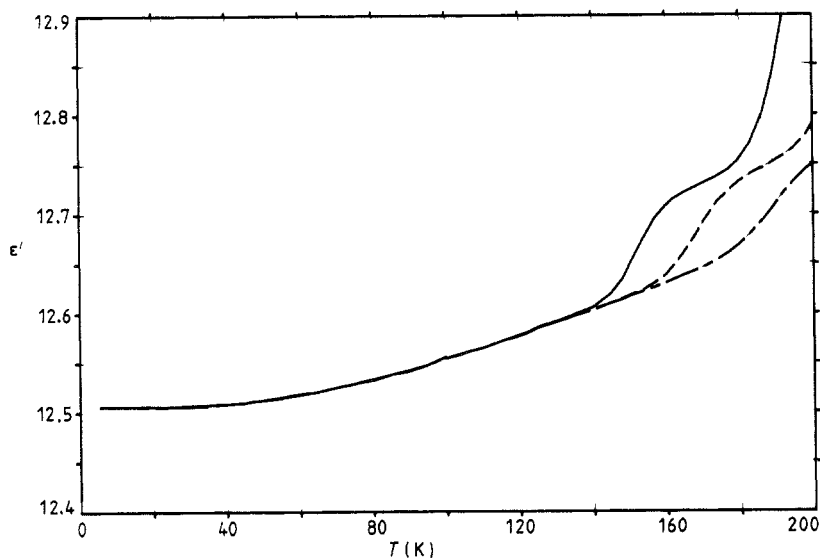

Figure 8. ε' against $T(K)$ parallel to the c axis for 0.03 mol% calcium-doped lanthanum trifluoride grown by Optovac, Inc. The curves connect the datum points and the curves from bottom to top are for 10^4, 10^3 and 10^2 Hz.

Acknowledgments

References

Andeen C, Schuele D and Fontanella J 1972 *Phys. Rev.* B **6** 591–5
Bailey A C and Yates B 1967 *Proc. Phys. Soc.* **91** 390–8
Barker A S Jr 1975 *Phys. Rev.* B **12** 4071–84
Chadwick A V, Hope D S, Jaroskiewicz G and Strange J H 1979 *Fast Ion Transport in Solids* ed. P Vashista, J N Mundy and G K Shenoy (Amsterdam: Elsevier–North-Holland)
Cochran W and Cowley R A 1962 *J. Phys. Chem. Solids* **23** 447–50
Figueroa D R, Chadwick A V and Strange J H 1978 *J. Phys. C: Solid State Phys.* **11** 55–73
Fontanella J, Andeen C and Schuele D 1972 *Phys. Rev.* B **6** 582–90
Fontanella J J, Chadwick A V, Carr V M, Wintersgill M C and Andeen C G 1980 *J. Phys. C: Solid State Phys.* **13** 3457–66
Fontanella J J, Wintersgill M C, Chadwick A V, Saghafian R and Andeen C G 1981a *J. Phys. C: Solid State Phys.* **14** 2451–64
Fontanella J J, Wintersgill M C, Welcher P J, Chadwick A V and Andeen C G 1981b *Solid State Ionics* **5** 585–8
Goldman M and Shen L 1966 *Phys. Rev.* **144** 321–31
Kimble R J Jr, Welcher P J, Fontanella J J, Wintersgill M C and Andeen C G 1982 *J. Phys. C: Solid State Phys.* **15** 3441–53
Kurosawa T 1961 *J. Phys. Soc. Japan* **16** 1298–308
Lee K and Sher A 1965 *Phys. Rev. Lett.* **14** 1027–9
Lowndes R R, Parrish J F and Perry C H 1969 *Phys. Rev.* **182** 913–22
Mooney J B 1966 *Infrared Phys.* **6** 153–7
Nowick A S 1967 *Adv. Phys.* **16** 1–47
Schoonman J, Oversluizen G and Wapenaar K E D 1980 *Solid State Ionics* **1** 211–21
Shannon R D 1976 *Acta Crystallogr.* A **32** 751–67
Sher A, Solomon R, Lee K and Muller M W 1966 *Phys. Rev.* **144** 593–604
——— 1967 *Lattice Defects and Their Interactions* ed. R R Hasigu (New York: Gordon and Breach)
Smyth C P 1955 *Dielectric Behaviour and Structure* (New York: McGraw-Hill)
Solomon R, Sher A and Muller M W 1966 *J. Appl. Phys.* **37** 3427–32
Swanson H E, Gilfrich N T and Cook M I 1957 *NBS Circular 539* vol 7 (Washington DC: US Government Printing Office) p 21
Wintersgill M C, Fontanella J J, Saghafian R, Chadwick A V and Andeen C G 1980 *J. Phys. C: Solid State Phys.* **13** 6525–36
Zalkin A, Templeton D H and Hopkins T E 1966 *Inorg. Chem.* **5** 1466–8